

Characteristics of $\text{Li}_{0.98}\text{Cu}_{0.01}\text{FePO}_4$ prepared from improved co-precipitation

Rong Yang^{a,b,*}, Xiaoping Song^a, Mingshu Zhao^a, Fei Wang^a

^a School of Science, Xi'an Jiao Tong University, Xi'an 710049, China

^b School of Science, Xi'an University of Technology, Xi'an 710048, China

Received 6 August 2007; received in revised form 21 December 2007; accepted 3 January 2008

Available online 4 March 2008

Abstract

Pure lithium iron phosphates and stoichiometric Cu-doped lithium iron phosphates were synthesized via improved co-precipitation, followed by sintering at high temperature for crystallization. The improved co-precipitation process allowed the homogeneous mixing of the ingredient reactants at atomic level. All samples were pure single phase indexed with orthorhombic *Pnmb* space group. The particle size of the $\text{Li}_{0.98}\text{Cu}_{0.01}\text{FePO}_4$ was drastically fine with 100–200 nm, compared with the undoped LiFePO_4 . The electrochemical performance of $\text{Li}_{0.98}\text{Cu}_{0.01}\text{FePO}_4$, including reversible capacity, cycle number and charge–discharge characteristics, exhibited better than those of LiFePO_4 .

© 2008 Elsevier B.V. All rights reserved.

Keywords: Lithium-ion batteries; Cathode material; Lithium iron phosphates; Ion doping

1. Introduction

Among cathode candidates, LiCoO_2 , LiNiO_2 and LiMn_2O_4 spinel have been widely used as cathode materials in lithium-ion batteries currently. More recently, LiFePO_4 has become one of the most promising compounds due to the relative lack of toxicity and inexpensive and abundant raw materials [1–5]. LiFePO_4 has a high lithium intercalation voltage of 3.4 V versus lithium metal and a high theoretical capacity of 170 mAh g^{-1} . However, there are two drawbacks for the use of LiFePO_4 as a commercial cathode material. One is its poor electronic conductivity [1]. Another problem is that it is difficult to synthesize LiFePO_4 because of iron oxidation state [6].

It is an effective method to improve electrochemical property of LiFePO_4 by supervalent ion doping and carbon coating [7–16]. Comparatively, volumetric capacity of cell is difficult to increase because the addition of carbon will decrease the practical density of cathode material. And the doping of 1% supervalent ion will hardly change the practical density of cathode material. Therefore, this mean will promote the prac-

tical utilization of LiFePO_4 . Chung et al. [7,8] proposed that LiFePO_4 doped with high valence metal ions could improve its electronic conductivity as high as eight orders of magnitude. Shi et al. [9,10] not only proved the feasibility of Cr^{3+} ion doping LiFePO_4 in theory, but also synthesized the sample. Wen et al. [17] also investigated the structure and properties of $\text{LiFe}_{0.9}\text{V}_{0.1}\text{PO}_4$ and indicated that the cathode properties of $\text{LiFe}_{0.9}\text{V}_{0.1}\text{PO}_4$, including reversible capacity, cycle number and charge–discharge characteristics, were better than those of pure LiFePO_4 . Moreover, it was not easy to dope ion uniformly by solid phase confused with 1.0% (molar ratio) ion, which may limit the function of doping. In present investigation, we are trying to put forward an improved co-precipitation route to prepare ion-doped LiFePO_4 . In this method, olivine LiFePO_4 will be gained by the precursor which was prepared by co-precipitation sintered in the N_2 , in which inexpensive and stable Fe^{3+} compound was used as raw material and inert gas was not used during the processes of co-precipitation. It is convenient to operate according to this preparation method with the purpose of industrial manufacture.

2. Experimental

The pure LiFePO_4 and doped $\text{Li}_{1-x}\text{Cu}_x\text{FePO}_4$ were synthesized by improved co-precipitation, followed by sintering at high temperature. The ingre-

* Corresponding author at: School of Science, Xi'an Jiao Tong University, Xi'an 710049, China. Tel.: +86 29 82066360; fax: +86 29 82066361.

E-mail address: yangrong8622@yahoo.com.cn (R. Yang).

dient chemicals LiOH (A.R, China), iron (III) sulfate $\text{Fe}_2(\text{SO}_4)_3 \cdot 7\text{H}_2\text{O}$ (A.R, China), $\text{NH}_4\text{H}_2\text{PO}_4$ (A.R, China) and $\text{CuSO}_4 \cdot 5\text{H}_2\text{O}$ (A.R, China) were dissolved in de-ionized water and proper ascorbic acid was added to form a homogeneous solution. A pH electrode would be inserted in solution and the pH was adjusted to 6 with ammonia water during the experiment. In the solution, Li^+ , Cu^{2+} , Fe^{2+} , $[\text{SO}_4]^{2-}$, and $[\text{PO}_4]^{3-}$ ions were mixed on molecular level. By stirring at 50°C for 1 h, lime precipitation was obtained from the solution. The optimum aging condition was 30 min, 60°C . After filtration, the precursor powders were transferred to furnace and sintered at 600°C for 10 h (N_2 atmosphere), and then allowed to cool slowly to room temperature.

The pure LiFePO_4 and doped $\text{Li}_{0.98}\text{Cu}_{0.01}\text{FePO}_4$ were characterized by SEM and X-ray diffraction. The SEM observation was performed on a JSM-5610 scanning electron microscope. The X-ray diffraction was carried out by using a Rigaku-D/MAX-2400 diffractometer with Cu K α radiation ($\lambda = 0.15406 \text{ nm}$).

The testing electrodes were made by dispersing 80 wt.% active materials, 15 wt.% acetylene black and 5 wt.% polyvinylidene fluoride (PVDF) binder in dimethyl phthalate solvent to form a slurry. Then the slurry was spread on to an aluminium foil and dried in the vacuum oven. The separator was a Celgard 2400 microporous membrane. 1M LiPF_6 solution in ethylene carbonate (EC)–dimethyl carbonate (DMC; 1:1 in volume) and lithium foil were used as an electrolyte and an anode respectively. The assembly of the cell prototypes was carried out in a dry glove box, under argon. The cathode performance was investigated in term of charge–discharge curves and cycle life. These tests were run by an Abin instrument BT-2000 between 2.5 and 4.0 V versus Li/Li^+ at room temperature (25°C). Cyclic voltammograms (CVs) were measured at a scan rate of 0.05 mV s^{-1} using an electrochemical workstation (Shanghai Chenhua Instrument Co. Ltd., China).

3. Results and discussion

The chemical compositions of Cu-doped lithium iron phosphates were analyzed by atomic absorption spectrometry. Determination of Fe^{2+} from the samples by spectrophotometry showed up to 99.95% of total iron, and the Fe^{2+} was hardly oxidized.

Fig. 1 shows that among all samples prepared, the discharge specific capacity of $\text{Li}_{0.98}\text{Cu}_{0.01}\text{FePO}_4$ is better than others. That is, the small amounts of Cu^{2+} doped are benefit to the increase of specific capacities.

The X-ray diffraction profiles of $\text{Li}_{0.98}\text{Cu}_{0.01}\text{FePO}_4$ are shown in Fig. 1. The sample is pure single phase indexed with orthorhombic $Pnmb$ space group. During the synthesis process, the ingredient ions Li^+ , Cu^{2+} , Fe^{2+} , and $[\text{PO}_4]^{3-}$ are homoge-

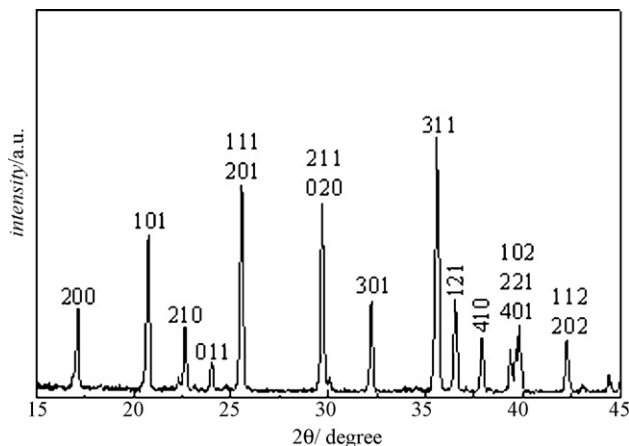


Fig. 2. XRD patterns of $\text{Li}_{0.98}\text{Cu}_{0.01}\text{FePO}_4$ sample.

neously mixed in atomic level. The precursor powders contain uniformly distributed reactants. After sintering, the pure lithium phospho-olivine structure is formed for Cu-doped lithium iron phosphates. No second phase is found as there are small amount of doped ion and doped ion exist in the form of solid-solution.

The lattice parameters of samples calculated from the XRD patterns (Fig. 2) are shown in Table 1.

From Table 1, we can see that the unit-cell parameter and unit-cell volume of LiFePO_4 doped by 1% Cu^{2+} has changed obviously, that is, the length of a -axis, b -axis and c -axis and unit-cell volume are both decreased. It shows that, compared with the pure LiFePO_4 , the unit-cell parameter and unit-cell volumes of $\text{Li}_{0.98}\text{Cu}_{0.01}\text{FePO}_4$ are both shrunk. The reason is that the ion radius of Cu^{2+} is 0.073 nm and smaller than 0.076 nm , that of Li^+ and it caused the decrease of length of c -axis. Another reason is that the binding force between Cu^{2+} and O^{2-} is larger than that between Li^+ and O^{2-} and the unit-cell volume of $\text{Li}_{0.98}\text{Cu}_{0.01}\text{FePO}_4$ shrunk. These reasons cause the change of charge–discharge characteristics.

The SEM image in Fig. 3(a) illustrates that the grains of the precursor are small and uniform, whose grain size is about $10 \mu\text{m}$. The precursor is the coexisting of two different crystallized shapes of particles. One shape is sector with the size of $3 \mu\text{m}$ and another is plush spherical with the size of $10 \mu\text{m}$. The particles size which grained from solid-state grinding were about $80 \mu\text{m}$, whereas the particles size which grained from improved co-precipitation were about $10 \mu\text{m}$ and uniform.

SEM images of LiFePO_4 and $\text{Li}_{0.98}\text{Cu}_{0.01}\text{FePO}_4$ samples are shown in Fig. 4. It is found that, after sintering at 600°C for 10 h, well-crystallized powders are obtained with an average crystal

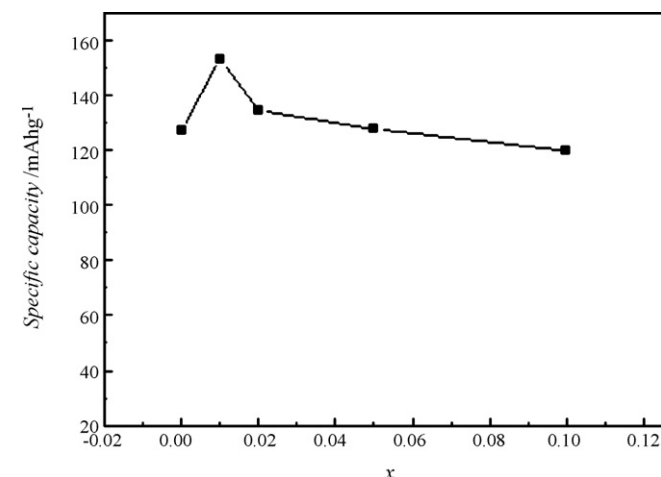


Fig. 1. Effect of quantity of Cu^{2+} doped on discharge specific capacity of samples.

Table 1
Lattice parameters of LiFePO_4 and $\text{Li}_{0.98}\text{Cu}_{0.01}\text{FePO}_4$

| Sample | a (nm) | b (nm) | c (nm) | V (nm^3) |
|---|-------------|-------------|-------------|-----------------------|
| LiFePO_4 | 1.033 | 0.6006 | 0.4687 | 0.2908 |
| $\text{Li}_{0.98}\text{Cu}_{0.01}\text{FePO}_4$ | 1.0316 | 0.6002 | 0.4682 | 0.2899 |
| Padhi et al. [1] | 1.0334 (4) | 0.6008 (3) | 0.4693 (1) | |
| Barker et al. [11] | 1.0288 | 0.5976 | 0.4672 | |
| Wen et al. [17] | 1.03155 (8) | 0.60032 (5) | 0.47011 (3) | 0.29112 (2) |

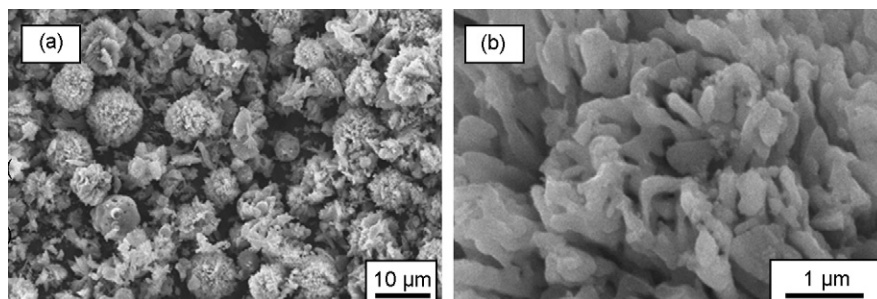


Fig. 3. SEM images of precursor making by co-precipitation: (a) skeleton diagram, $\times 1000$ and (b) $\times 20,000$.

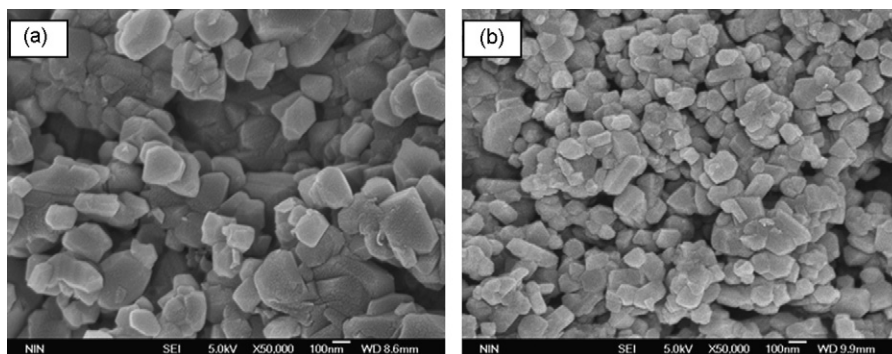


Fig. 4. SEM images of LiFePO_4 and $\text{Li}_{0.98}\text{Cu}_{0.01}\text{FePO}_4$ samples: (a) LiFePO_4 and (b) $\text{Li}_{0.98}\text{Cu}_{0.01}\text{FePO}_4$.

size of 300 nm of LiFePO_4 crystals (Fig. 4a) and another average crystal size of 100–200 nm of $\text{Li}_{0.98}\text{Cu}_{0.01}\text{FePO}_4$ crystals (Fig. 4b). The average size of $\text{Li}_{0.98}\text{Cu}_{0.01}\text{FePO}_4$ is fined evidently compared with that of LiFePO_4 . The small particle size of $\text{Li}_{0.98}\text{Cu}_{0.01}\text{FePO}_4$ would be beneficial to reduce the diffusion length of the lithium ion inside, resulting in fast reaction and diffusion kinetics, which can increase charge–discharge capacity and cycling behavior.

Fig. 5 illustrates EDS of $\text{Li}_{0.98}\text{Cu}_{0.01}\text{FePO}_4$. It could verify the homogeneous existence of Cu^{2+} dopant in LiFePO_4 crystal. It is a conceivable fact with the reason that the doping process of co-precipitation could undergoes in aqueous solution, which

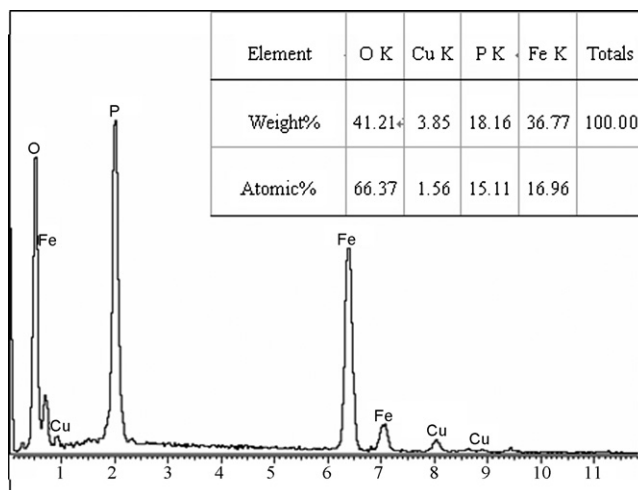


Fig. 5. EDS of $\text{Li}_{0.98}\text{Cu}_{0.01}\text{FePO}_4$.

can easily blend all soluble components uniformly even for low content ion dopant.

The charge/discharge curves are shown in Fig. 6. The cell is cycled between 2.5 and 4.0 V using a low current density of 0.1 C (17 mAh g^{-1}) at room temperature. $\text{Li}_{0.98}\text{Cu}_{0.01}\text{FePO}_4$ demonstrates a flatter charging and discharging plateau than that of pure LiFePO_4 . The potential for charging is about 3.49 V and discharging potential is around 3.37 V, which is in consistent with the result from the CV test. The small voltage difference between the charge/discharge plateaus is representative of its good kinetics. The discharge capacities stay at 153 mAh g^{-1} .

Fig. 7 shows the cyclic voltammogram of a $\text{Li}_{0.98}\text{Cu}_{0.01}\text{FePO}_4$ electrode at a scanning rate of 0.05 mV s^{-1} . The anodic and cathodic peaks appeared in the CV curves correspond to the two-phase charge–discharge reaction of the $\text{Fe}^{2+}/\text{Fe}^{3+}$ redox couple. During anodic sweep, the lithium ions were extracted from Li_xFePO_4 structure. An oxidation peak formed at 3.51 V during scanning potential from 4.0 to 2.8 V when lithium ions inserted into Li_xFePO_4 structure. The corresponding reduction peaks formed at 3.32 V. The 0.29 V difference between the anodic and cathodic peaks is representative of its good kinetics. Hence, the sharp oxidation and reduction peaks in CV curves indicate that strong lithium intercalation and de-intercalation reactions occurred for $\text{Li}_{0.98}\text{Cu}_{0.01}\text{FePO}_4$ electrode.

To investigate the rate capability, cycle performance of $\text{Li}_{0.98}\text{Cu}_{0.01}\text{FePO}_4$ at various rates is shown in Fig. 8. Although the discharge specific capacity has decreased with increasing charge/discharge rate, the capacity retention remained very good for all the different rates. At 0.1 C, the discharge capacity decreased from 154.5 to 140.9 mAh g^{-1} . The capacity decreased

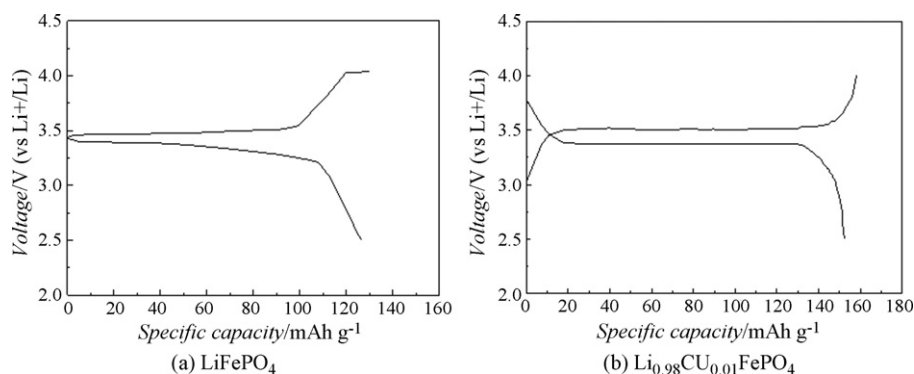


Fig. 6. The initial charge/discharge curves of LiFePO_4 and $\text{Li}_{0.98}\text{Cu}_{0.01}\text{FePO}_4$ sample at 0.1 C-rate.

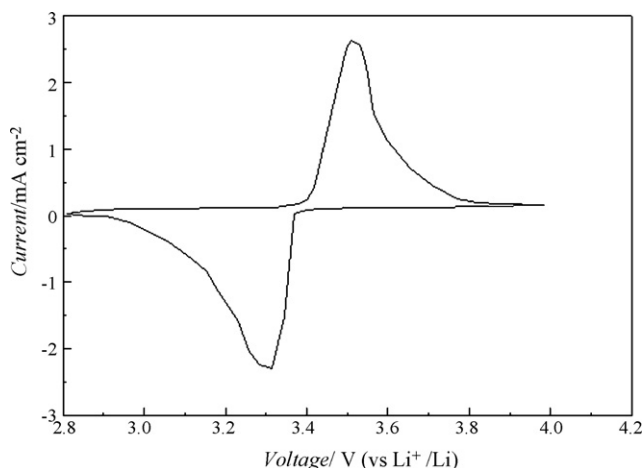


Fig. 7. Cyclic voltammetry curves of $\text{Li}_{0.98}\text{Cu}_{0.01}\text{FePO}_4$.

to 139.0 mAh g^{-1} (1 C) and 130.2 mAh g^{-1} (2 C) at the current densities increase. At higher discharge rate of 2 C, the cell could deliver a capacity of 120.1 mAh g^{-1} after 30 cycle. As a whole, the capacities of $\text{Li}_{0.98}\text{Cu}_{0.01}\text{FePO}_4$ seem to be stable upon cycling.

Above results which demonstrated good rate performance and cycling stability of $\text{Li}_{0.98}\text{Cu}_{0.01}\text{FePO}_4$ could be attributed to the fact that the small particle size distribution and improved

conductivity through doping Cu^{2+} . Especially, after substitution, balance of electrical valence induced Li^+ defect in LiFePO_4 and residue of $\text{Fe}^{2+}/\text{Fe}^{3+}$ coexistence state, so cation defects are of benefit to the diffusion of Li^+ in solid phase and increase electrical conductivity of crystal, further the charge–discharge characteristics of material.

4. Conclusion

The lithium iron phosphate and its doped derivatives have been successfully synthesized by improved co-precipitation. Cu^{2+} uniform distribution in LiFePO_4 crystal and lead no impurity growth. The Cu-doped lithium iron phosphates demonstrated a better electrochemical property in terms of capacity delivery, cycle performance and electrochemical reversibility, which is attributed to the enhancement of the electronic inductivity by ion dopant, compared with undoped LiFePO_4 . And small size of $\text{Li}_{0.98}\text{Cu}_{0.01}\text{FePO}_4$ synthesized by improved co-precipitation may allow intercalation and de-intercalation of lithium ions to occur with ease during the charge–discharge processes and exhibit high discharge capacity and good reversibility. Ion-doped samples show that such ion doping by the improved co-precipitation is an effective method to improve the electrochemical performance of LiFePO_4 .

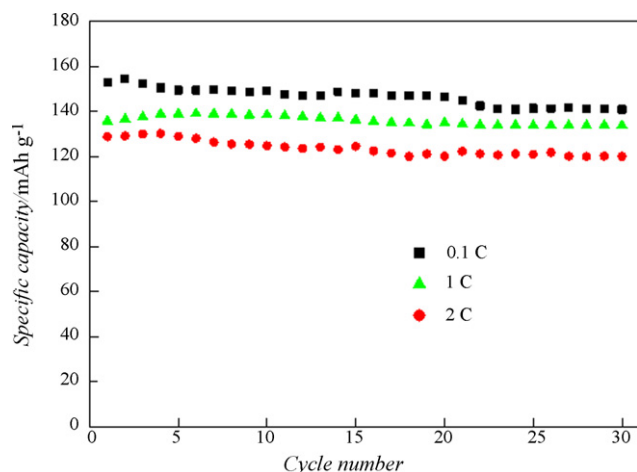


Fig. 8. Cycle life curves of $\text{Li}_{0.98}\text{Cu}_{0.01}\text{FePO}_4$ sample.

References

- [1] A.K. Padhi, K.S. Nanjundaswamy, J.B. Goodenough, *J. Electrochem. Soc.* 144 (1997) 1188.
- [2] M. Thackeray, *Nat. Mater.* 1 (2002) 81.
- [3] A.K. Padhi, K.S. Nanjundaswamy, C. Masquelier, S. Okada, J.B. Goodenough, *J. Electrochem. Soc.* 144 (1997) 1609.
- [4] S.L. Bewlay, K. Konstantinov, G.X. Wang, S.X. Dou, H.K. Liu, *Mater. Lett.* 58 (2004) 1788.
- [5] C.H. Mi, G.S. Cao, X.B. Zhao, *Mater. Lett.* 59 (2005) 127.
- [6] S. Franger, F.L. Cras, C. Bourbon, H. Rouault, *J. Power Sour.* 119–121 (2003) 252.
- [7] S.Y. Chung, J.T. Bloking, Y.M. Chiang, *Nat. Mater.* 1 (2002) 123.
- [8] S.Y. Chung, Y.M. Chiang, *Electrochem. Solid-State Lett.* 6 (2003) A278.
- [9] S.Q. Shi, L.J. Liu, C.Y. Ouyang, D.S. Wang, Z.X. Wang, L.Q. Chen, X.J. Huang, *Phys. Rev. B* 68 (2003) 195.
- [10] C.Y. Ouyang, S.Q. Shi, Z.X. Wang, H. Li, X.J. Huang, L.Q. Chen, *J. Phys. Condens. Mater.* 16 (2004) 2265.
- [11] J. Barker, M.Y. Saidi, J.L. Swoyer, *J. Electrochem. Soc.* 6 (2003) A53.

- [12] S. Franger, F.L. Cras, C. Bourbon, H. Rounault, *Electrochem. Solid-State Lett.* 5 (2002) A231.
- [13] S.T. Myung, S. Komaba, N. Hirosaki, H. Yashiro, N. Kumagai, *Electrochim. Acta* 49 (2004) 4213.
- [14] P.P. Prosini, M. Carewska, S. Scaccia, P. Wisniewski, S. Passerini, M. Pasquali, *J. Electrochem. Soc.* 149 (2002) A886.
- [15] M.A.E. Sanchez, G.E.S. Brito, M.C.A. Fantini, G.F. Goya, J.R. Matos, *Solid State Ionics* 177 (2006) 497.
- [16] H. Gabrisch, J.D. Wilcox, M.M. Doeff, *Electrochem. Solid-State Lett.* 9 (2006) A360.
- [17] Y.X. Wen, L.M. Zeng, Zh.F. Tong, L.Q. Nong, W.X. Wei, *J. Alloys Compd.* 416 (2006) 206.